ACS Biomaterials SCIENCE & ENGINEERING

pubs.acs.org/journal/abseba Article

Protein-Based Films Functionalized with a Truncated Antimicrobial Peptide Sequence Display Broad Antimicrobial Activity

André da Costa,* Ana M. Pereira, Paula Sampaio, José Carlos Rodríguez-Cabello, Andreia C. Gomes, Margarida Casal, and Raul Machado*

Cite This: https://dx.doi.org/10.1021/acsbiomaterials.0c01262 Read Online

ACCESS | Metrics & More | Article Recommendations | Supporting Information

ABSTRACT: The increasing bacterial resistance to antibiotics is driving strong demand for new antimicrobial biomaterials. This work describes the fabrication of free-standing films exhibiting antimicrobial properties by combining, in the same polypeptide chain, an elastin-like recombinamer comprising 200 repetitions of the pentamer VPAVG (A200) and an 18-amino-acid truncated variant of the antimicrobial peptide BMAP-28, termed BMAP-18. The fusion protein BMAP-18A200 was overexpressed and conveniently purified by a simplified and scalable nonchromatographic process. Free-standing films of BMAP-18A200 demonstrated to be stable without requiring cross-linking agents and displayed high antimicrobial activity against skin pathogens including Gram-negative and Gram-positive bacteria as well as unicellular and filamentous fungi. The antimicrobial activity of the films was mediated by direct contact of cells with the film surface, resulting in compromised structural integrity of microbial cells. Furthermore, the BMAP-18A200 films showed no cytotoxicity on normal human cell lines (skin fibroblasts and keratinocytes). All of these results highlight the potential of these biotechnological multifunctional polymers as new drug-free materials to prevent and treat microbial infections.

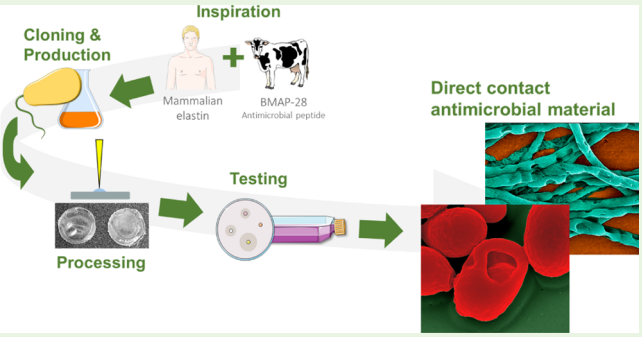

KEYWORDS: *antimicrobial peptides, antimicrobial materials, elastin-like recombinamers, multifunctional materials, skin infections*

■ INTRODUCTION

The increase in antimicrobial resistance to antibiotics is a major challenge representing one of the biggest threats to global health not only due to the appearance of super-resistant microbes but also due to the low pace in discovery of new and efficient antibiotics.[1,2] As a result, standard treatments for bacterial infections are gradually becoming ineffective.

New research discloses the potential use of antimicrobial peptides (AMPs) as promising biocide alternatives.[3,4] These small molecular weight peptides are part of the innate immunity of various organisms and are characterized by an amphipathic structure and positive net charge. A remarkable property of AMPs is the broad activity against bacteria, fungi, viruses, parasites, and even cancer cells.[5,6] Due to their ancestral origin and mode of action, AMPs are less prone to elicit antimicrobial resistance response in comparison to classical antibiotics: they target very conserved structures like components of the cell wall, plasma membrane, or genetic material.[5,7] These characteristics make AMPs promising biotechnological tools for the development and functionalization of innovative healthcare-associated materials and devices with broad biocide properties.

Despite their potential and auspicious properties, the successful exploitation of AMPs still remains challenging. The direct isolation of AMPs from natural sources is useful for initial characterization studies but is extremely laborious and expensive, usually resulting in low yields and impure products. An alternative way to obtain AMPs with high purity is through chemical synthesis. However, the high costs associated with the synthesis process and the possibility of introducing errors into the sequence limits production upscaling. Compared with these two strategies, the use of recombinant DNA technology for the production of AMPs presents advantages such as low production costs, high productivity associated with short production periods, and relatively simple purification processes with high yields.[8,9] Nevertheless, the heterologous expression of AMPs is challenging as these are toxic to the producing host and susceptible to proteolytic degradation. Fusion proteins are normally used for the expression of AMPs, protecting cells from toxicity and proteolysis, with some strategies involving the production as inclusion bodies.[10,11]

Received: August 26, 2020
Accepted: January 13, 2021

A promising strategy for the biotechnological production of AMPs is their combination with bioengineered recombinant protein-based polymers, such as elastin-like recombinamers (ELRs).[12−14] This strategy allows using ELRs not only as production and purification tags through ITC (inverse transition cycling) employing simple hot and cold cycles,[12,15−17] but also as a structural matrix for the development of antimicrobial materials.[13,14] ELRs are based on the mammalian tropoelastin sequence[18] and are of particular interest due to their reversible temperature-dependent phase-transitional behavior[18,19] and good biocompatibility.[20−22] Composed of 200 repetitions of the pentamer VPAVG, the bioengineered polymer A200 used in this work is an ELR that reveals thermal hysteresis,[23,24] self-assembling into spherical sub-microparticles at temperatures above 33 °C and only disassembling when the temperature is strongly cooled to ∼12 °C.[13,23] This allows one to obtain stable materials over a wide range of temperatures and without further cross-linking, which can be explored for different applications in the biomedical and biotechnological fields.[14,25,26]

BMAP-28 (bovine myeloid antimicrobial peptide-28) is an α-helical peptide with 28 amino acids that belongs to the cathelicidin family of peptides and display potent activity against Gram-positive and Gram-negative bacteria as well as fungi, giving good indications for its use in the development of antimicrobial materials.[27−30] BMAP-28 does, however, induce cytotoxicity in certain human cell types limiting its potential biomedical application.[28,31] This toxic effect is associated with the hydrophobic C-terminal tail of BMAP-28, and therefore, cytotoxicity to mammalian cells can be greatly reduced by shortening the peptide at the C-terminus.[32] Skerlavaj et al. demonstrated that chemically synthesized truncated variants of the cathelicidins precursors BMAP-28 and BMAP-27, consisting of the first 1−18 amino acid residues of the N-terminus, show a dramatic reduction in the lytic activity on mammalian cells while maintaining a very potent antimicrobial activity with a wide spectrum.[32]

In this work, we report the recombinant synthesis of the 1−18 amino acid truncated derivative of BMAP-28 (termed BMAP-18) fused to A200 to create an all-protein antimicrobial material. We demonstrate how to process the BMAP-18A200 into new biotechnological antimicrobial materials for skin-related applications. We envisage that the strategy of combining AMPs with ELR-based proteins sets the basis for the development of a platform to engineer new multifunctional antimicrobial materials.

■ MATERIAL AND METHODS

Cloning and Protein Production. BMAP-18A200 DNA sequence was obtained by common genetic engineering methodologies using codon usage-optimized DNA sequences for *Escherichia coli*. All of the obtained constructs were verified by DNA sequencing (Eurofins). Following the work by Skerlavaj,[32] the genetic sequence of BMAP-28[33] was used as a template to design the 1−18 truncated variant. For the construction of BMAP-18A200, the genetic sequence with flanking *Nde*I and *Kpn*I restriction sites (for compatibility with A200) coding for the first 18 amino acids of BMAP-28 was amplified by PCR and ligated with the N-terminus of A200 previously cloned into an adapted pET25b(+) (Novagen) expression plasmid[23] (Supporting Figure S1). The final expression vector was transformed into *Escherichia coli* strain BL21(DE3) and utilized for protein expression in autoinduction conditions (Terrific Broth supplemented with α-lactose; yeast extract 24 g, K_2HPO_4 12.54 g, tryptone 12 g, glycerol 5.04 g, KH_2PO_4 2.31 g, lactose 2 g, kanamycin 50 mg/L) at 200 rpm for 22 h at 37 °C. Protein purification of BMAP-18A200 (87 kDa) was achieved by ITC as described elsewhere.[13,16]

Characterization of Protein Polymer Solutions. Differential scanning calorimetry (DSC) studies were performed on a Mettler Toledo DSC 822e. The enthalpy and temperature calibration were performed using standard indium and zinc samples. Standard 40 μL aluminum pans were used with 20 μL of each polymer solution at 25 mg/mL in mQ water or phosphate-buffered saline (PBS) (NaCl 8 g, Na_2HPO_4 1.44 g, KH_2PO_4 0.24 g, KCl 0.2 g/L, at pH 7.4). A program with four stages was devised for each sample: (i) 5 min isothermal stage at 0 °C; (ii) 5 °C/min heating stage from 0 °C to 50 °C; (iii) 5 min isothermal stage at 50 °C; and (iv) 5 °C/min cooling stage from 50 to 0 °C. Analysis of thermograms and determination of peak and onset temperatures were accomplished using STARe and OriginPro 8.1 (OriginLab, Northampton, MA).

Characterization of the self-assembled structures was achieved through size and ζ-potential measurements at different protein-polymer concentrations (0.001, 0.01, and 0.1 mg/mL) in mQ water or PBS. All of the assays were performed on a Zetasizer Nano ZSP (Malvern) equipment at 37 °C with a 3 min equilibration time. The size average was calculated considering 15 measurements at a defined 173° backscatter angle. The analysis was completed with Zetasizer Software (Malvern).

In circular dichroism (CD) experiments, 10 μM BMAP-18A200 in phosphate buffer (5 mM potassium phosphate, pH 7.4) was analyzed in a Jasco J-1500 Circular Dichroism Spectrophotometer equipped with a Peltier element. The obtained spectra were the result of three cumulative measurements in the wavelength range of 190−260 nm, at a scanning speed of 20 nm/min in continuous mode and a resolution of 1.0 nm, at both 20 and 37 °C. The estimation of the percentage of secondary structures was performed with the BestSel algorithm.[34]

Antimicrobial Activity of Protein Solutions. Antimicrobial activity assays were performed using an adapted version of the Kirby-Bauer agar diffusion method with Lysogeny broth (LB: tryptone 10 g, yeast extract 5 g, sodium chloride 5 g, per liter)[16] following CLSI recommendations. Holes were made in the LB medium−agar (1.5% w/v) plates using an inverted sterile Pasteur pipette. The holes were filled with 25 μL of BMAP18-A200 at 10% (w/v) concentration in a 0.87% NaCl solution, supplemented with 0.05% acetic acid, corresponding to 2.5 mg of the protein polymer or 60 μg of AMP. Overnight cultures of *Bacillus subtilis* 48886, *E. coli* HB101, *Pseudomonas aeruginosa* ATCC10145, and *Staphylococcus aureus* ATCC6538 were diluted to a final cell density of 1×10^6 cells/mL in LB medium−agar (0.8% w/v) and layered on the top of the LB plates. Saline solution (25 μL) was used as a negative control, and discs saturated with kanamycin (30 μg, BD Biosciences) was used as a positive control for growth inhibition. After overnight incubation at 37 °C, the growth inhibitory zones were visually inspected and their respective diameters were measured using *ImageJ* software.[35]

Preparation of Free-Standing Films. BMAP-18A200 (10% w/v) in formic acid (98−100%, Merck) solutions were prepared and used for solvent casting. Films were obtained by casting the protein solution on poly(tetrafluoroethylene) (PTFE) casting molds with 10 mm diameter followed by solvent evaporation at room temperature under fume hood extraction. After solvent evaporation, the obtained films were carefully peeled off and sterilized by UV exposure (20 min) before use in subsequent experiments.

Film Characterization. Attenuated total reflectance-Fourier transform infrared (ATR-FTIR) analysis was performed at room temperature in a Spectrum Two spectrometer (Perkin Elmer) with a deuterated triglycine sulfate (DTGS) detector and KBr beam splitter coupled with a UATR accessory (single reflection diamond, Perkin Elmer). Spectra were represented as the accumulation of 64 scans with a resolution of 4 cm^{-1}.

Thermal analysis of BMAP-18A200 films was performed by DSC (Mettler Toledo DSC822^e) from 30 to 200 °C with a constant heating rate of +10 °C/min and analyzed with OriginPro 8.1 (OriginLab, Northampton, MA).

https://dx.doi.org/10.1021/acsbiomaterials.0c01262
ACS Biomater. Sci. Eng. XXXX, XXX, XXX−XXX

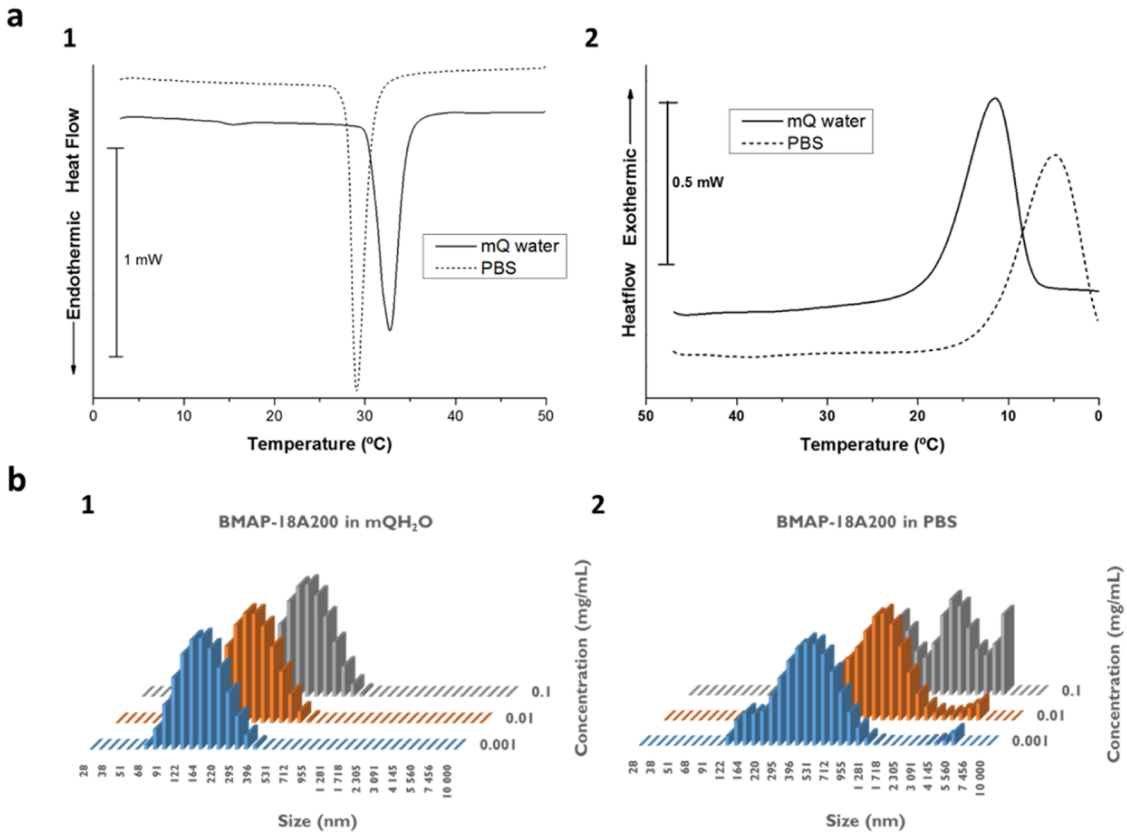

Polymer concentration (mg/mL)	Z-average (nm)	PDI
0.001	151 (±3)	0.124 (± 0.030)
0.01	225 (± 7)	0.113 (±0.019)
0.1	358 (± 17)	0.113 (±0.027)

Polymer concentration (mg/mL)	Z-average (nm)	PDI
0.001	484 (±142)	0.281 (± 0.048)
0.01	1088 (± 409)	0.289 (±0.095)
0.1	2783 (± 1187)	0.338 (±0.114)

Figure 1. Thermal behavior and self-assembling properties of BMAP-18A200. (a) DSC thermograms of BMAP-18A200 in mQ water and PBS during the (1) heating stage and the (2) cooling stage. (b) Dynamic light scattering analysis (DLS) of BMAP-18A200 dissolved in (1) mQ water and (2) PBS at different concentrations, and respective tables with values for size (Z-average) and polydispersity index (PDI).

Water contact angle (WCA) measurements were performed in a Data Physics OCA15 device at room temperature using a sessile drop in dynamic mode and mQ water as testing liquid. Measurement of contact angles was performed after deposition of 0.5 μL water drops on the sample surface and analyzed with the manufacturer's software (SCA20). WCA values were determined as the average of at least 3 measurements in different zones of the film.

Transmittance (%T) of BMAP-18A200 films was assessed in the range of 350−1000 nm at room temperature. Film surface analysis was carried out by atomic force microscopy (AFM) and scanning electron microscopy (SEM). For SEM observation, film samples were coated with a thin Au/Pd layer using a sputter coater and visualized in a NanoSEM−FEI Nova 200. Surface roughness (Ra) was determined by AFM as the average of two samples using a Dimension Icon (Bruker) atomic force microscope in the ScanAsyst mode using ScanAsyst air probes at 1 Hz and a scanning area of 5 μm × 5 μm.

Evaluation of Antimicrobial Activity. The antimicrobial activity of BMAP-18A200 free-standing films was investigated by direct contact using a protocol based on the ISO 22196 guidelines, as previously described.[13] Briefly, a cell suspension (50 μL) containing 1 × 10^6 CFUs/mL of bacterial cells or 1 × 10^5 CFUs/mL of yeast cells was added to the surface of the films (10 mm diameter) and incubated for 2 h, at 37 °C for bacteria and 30 °C for yeasts, in 24 well plates. Following incubation time, 950 μL of sterile PBS was added, the plate agitated, and serial dilutions were plated on LB agar or YPD agar (agar 15 g, glucose 10 g, yeast extract 5 g, peptone 5 g, per liter) for bacteria or yeast CFUs enumeration, respectively. The bacterial species used in this study were as follows: *P. aeruginosa* ATCC 10145, *E. coli* HB101, *S. aureus* ATCC 6538, and a *Klebsiella pneumoniae* isolate. Yeast species included *Candida albicans* PYCC 3436, *Candida glabrata* CBS 138, *Candida parapsilosis* ATCC 22019, and *Saccharomyces cerevisiae* PYCC 4072. Polystyrene (PS) discs with 10 mm diameter were used as a control for 100% survival. Results were expressed as lethality percentage (% of kill) using eq 1

$$\%\ \text{of kill} = \frac{(\text{control CFUs} - \text{sample CFUs})}{\text{control CFUs}} \times 100 \quad (1)$$

The morphology of microbial cells after contact with BMAP-18A200 was qualitatively assessed by SEM. To do so, a cell suspension (50 μL) of bacteria and yeast (1 × 10^7 CFUs/mL) was deposited on the film surface for 120 min at 37 °C for bacteria or 30 °C for yeasts. Sterile 10 mm polystyrene (PS) discs were used as 100% survival control. For fixation, samples were immersed for 1 h at room temperature in 2.5% v/v glutaraldehyde in PBS solution and rinsed with water. The samples were then dehydrated through immersion in 0.5 mL of successive ethanol/water solutions (55.0, 70.0, 80.0, 90.0, 95.0, and 100.0% v/v of ethanol) for 30 min, dried in the fume hood, and analyzed by SEM (NanoSEM, FEI NOVA 200).

Antifungal assays were performed *in vitro* using the filamentous fungus *Aspergillus nidulans*. Briefly, a sterile toothpick was used to collect spores (conidia) and plated in complete medium (CM, salt solution 20 mL, vitamin solution 10 mL, glucose 10 g, peptone 2 g,

https://dx.doi.org/10.1021/acsbiomaterials.0c01262
ACS Biomater. Sci. Eng. XXXX, XXX, XXX−XXX

casamino acids 1 g, yeast extract 1 g, per liter at pH 6.8). BMAP-18A200 films were deposited on the agar near the spore inoculation sites, incubated at room temperature for 48 and 72 h, and digitally recorded (Chemidoc XRS system, Bio-Rad). As for SEM visualization, a spore germination assay was performed with an inoculum containing spores of *A. nidulans* placed in contact with BMAP-18A200 films and PS discs (negative control for antifungal activity) at 37 °C for 18 h. Likewise, an overnight grown *A. nidulans* hyphae were placed in contact with the top of BMAP-18A200 films for 18 h at 37 °C. Sample fixation and visualization were performed as previously described for bacteria and yeast samples.

Cytotoxicity. Cytotoxicity of BMAP-18A200 films by indirect contact was evaluated using human keratinocytes (NCTC 2544) and normal human skin fibroblasts (BJ-5ta, telomerase-immortalized) cell lines. Sterile BMAP-18A200 films were placed on 24-well plates (Nunclon, ThermoScientific) with 0.75 mL of cell culture medium and incubated for 24 h at 37 °C, 5% CO_2 in a humidified environment-conditioned medium. At the same time, 0.1 mL of cell suspension (6.6×10^4 cells/mL) was cultured for 24 h in surface-treated 96-well plates (Nunclon, Thermo Scientific). The culture medium was then replaced with the conditioned medium, and cell viability (measured in terms of metabolic activity) was evaluated after 24 and 72 h, by the MTS assay according to manufacturer's instructions (CellTiter 96 Aqueous One Solution Cell Proliferation, Promega). Cells grown in standard culture medium were used as positive control and set as 100% viability. Cells cultured in a culture medium with 30% dimethyl sulfoxide (DMSO) were used as a negative control for cell viability.

Statistical Analysis. Unpaired *t*-test with Welch's correction was carried with GraphPad Prism 5, assuming a p-value < 0.05 to be considered as statistically significant. All of the experiments were performed, at least, in triplicate.

RESULTS

Production of Recombinant BMAP-18A200. BMAP-18A200 was obtained by genetic engineering methods and successfully expressed in *E. coli* BL21(DE3) (see the Supporting Information for more details). Analysis of protein expression levels revealed a clear overexpression of BMAP-18A200 (MW 87 kDa) although at an apparent higher molecular weight than expected (Supporting Figure S1b). This abnormal gel mobility is attributed to the hydrophobic nature of the recombinant protein and has been previously observed for ELRs.[16,23,36] The protein was purified by ITC (Supporting Figure S2) leading to a final volumetric productivity of 108 mg/L.

Characterization of the Self-Assembly Behavior of BMAP-18A200. Differential scanning calorimetry (DSC) was applied to study the thermoresponsive behavior of BMAP-18A200 dissolved in mQ water and PBS, as well as to calculate its transition temperature (T_t) (Figure 1a). Figure 1a-1 depicts the thermograms obtained during the heating stage, showing an endothermic peak characteristic of the phase transition upon heating and associated with the self-assembling process of ELRs.[16,23] Accordingly, the transition temperatures were 32.7 and 29.0 °C (determined by the peak center) for the samples in mQ water and PBS, respectively. During the cooling stage, the exothermic peaks observed at 11.4 °C (sample in mQ water) and 4.9 °C (sample in PBS) correspond to the resolubilization of BMAP-18A200 due to the reversibility of the self-assembly process.[16,23]

Characterization of the self-assembled structures by dynamic light scattering (DLS) revealed a variation in the particle size depending on the concentration and solvent (Figure 1b). The *Z*-average values increased with concentration, ranging from 151 to 358 nm in mQ water and from 484 to 2783 nm in PBS. The samples in mQ water showed lower *Z*-average values than the samples in PBS. The polydispersity index (PDI) of the mQ water samples remained constant (around 0.1) regardless of concentration, indicating a homogenous population of self-assembled structures (Figure 1b-1). The samples in PBS showed an increase in PDI with increasing concentrations, reaching values of 0.28 for a concentration of 0.001 mg/mL and 0.338 for a concentration of 0.1 mg/mL, suggesting aggregation (Figure 1b-2). The ζ-potential of BMAP-18A200 in aqueous solution increases with increasing concentration, showing values of −2.39 (± 1.89), 3.20 (±1.29), and 13.2 (±3.00) mV for 0.001, 0.01, and 0.1 mg/mL, respectively. CD analysis of BMAP-18A200 in solution, below (20 °C) and above (37 °C) the transition temperature, clearly show the structural conformational changes attributed to the phase transition. Below the transition temperature, there is a predominance of antiparallel β-sheets (41%) and other structures (45%, including 310-helix, π-helix, β-bridge, bend, loop/irregular, and invisible regions of structure), and turns at a lower extent (14%) (Supporting Figure S3). At temperatures above 37 °C, there is a clear loss of the signal hampering a proper assessment of secondary content.

Antibacterial Activity of BMAP-18A200 in Solution. A modified Kirby-Bauer disc diffusion susceptibility test was performed to evaluate the antimicrobial activity of BMAP-18A200 in solution. In this assay, holes were pinched in agar plates where the sample solution was poured before placing the bacteria-containing top agar to cover the entire plate surface. Figure 2 shows the inhibition halo measurements obtained for

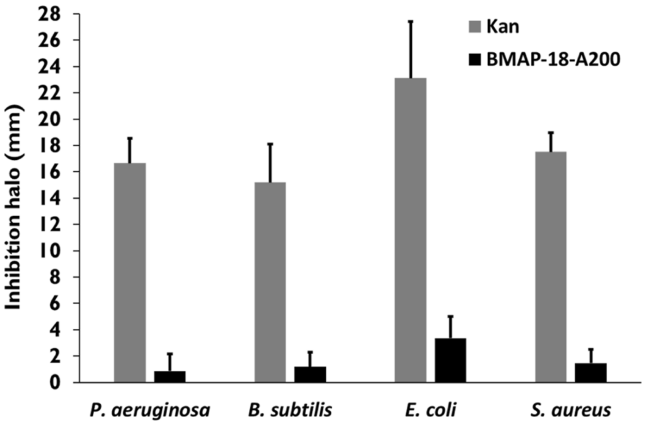

Figure 2. Antimicrobial activity of soluble BMAP-18A200 determined by measurement of the inhibition halo of 2.5 mg of BMAP18-A200 from a 10% w/v solution (corresponding to 60 μg of peptide BMAP-18) and 30 μg of kanamycin-impregnated discs.

BMAP-18A200 solution (2.5 mg) compared to the positive control kanamycin (30 μg). Results indicate that *E. coli* is the most susceptible species to BMAP-18A200, whereas, for *P. aeruginosa*, *S. aureus* (see Supporting Figure S4), and *B. subtilis* only marginal inhibition halos (under 2 mm) were observed.

Characterization of BMAP-18A200 Free-Standing Films. Optically transparent and structurally stable free-standing films of BMAP-18A200 (Supporting Figure S5) were obtained by solvent casting, using a 10% (w/v) concentration in formic acid. The films demonstrated to be optically transparent with transmittance values over 85% in the visible light spectrum region (400−750 nm). Topographical analysis by SEM and AFM revealed a smooth surface with

https://dx.doi.org/10.1021/acsbiomaterials.0c01262
ACS Biomater. Sci. Eng. XXXX, XXX, XXX−XXX

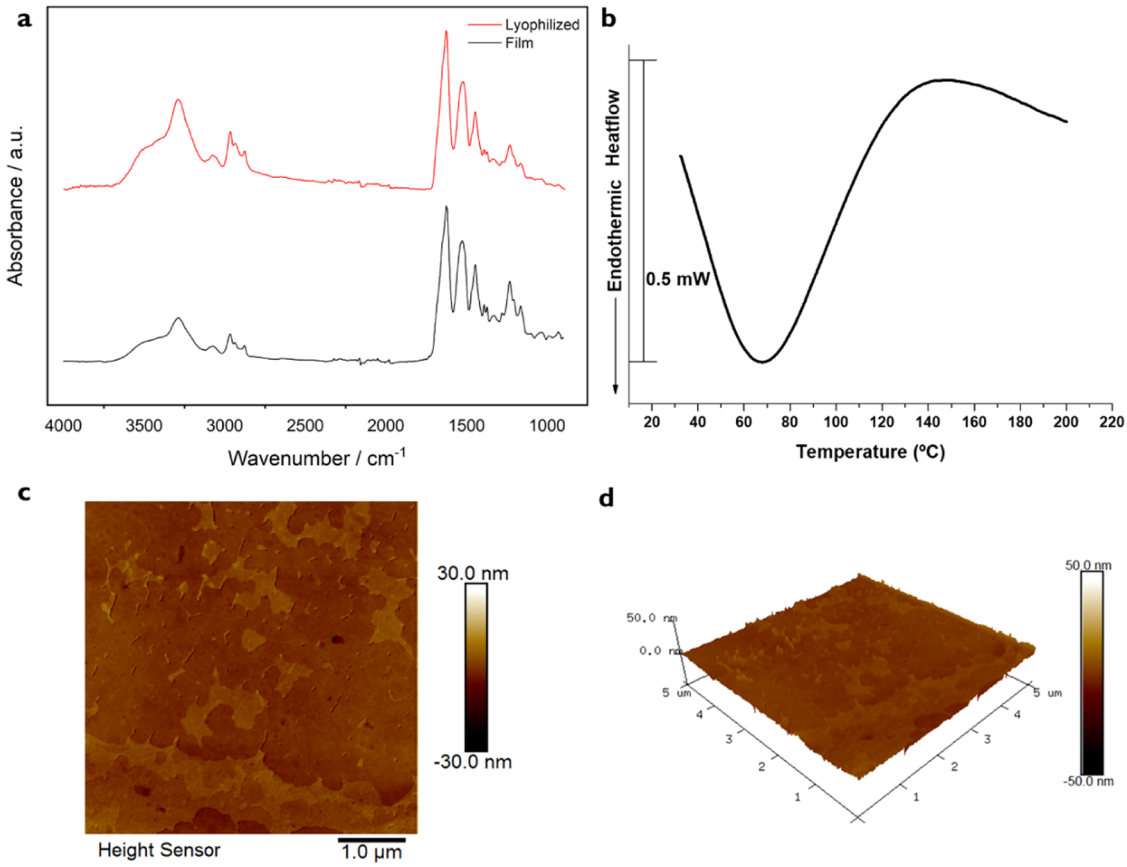

Figure 3. Characterization of BMAP-18A200 free-standing films: (a) ATR-FTIR spectra of lyophilized and film samples; (b) DSC thermogram; (c) AFM analysis of surface roughness for BMAP-18A200 films with a representative micrograph of a scanning area of 5 μm × 5 μm; and (d) its three-dimensional (3D) representation.

mean roughness (Ra) of 1.59 ± 0.13 nm (Supporting Figure S5 and Figure 3c,d).

Fourier-transformed infrared spectroscopy with attenuated total reflection mode (ATR-FTIR) was applied to study the structural conformation changes between lyophilized samples and cast films of BMAP-18A200. Both films and lyophilized samples present similar spectra with no noteworthy changes resulting from the processing by solvent casting (Figure 4a). The infrared spectra are characterized by the presence of an amide I peak (C═O stretching vibration) centered at 1626 cm^{-1} and minor dislocation of the amide II peak (N−H bending with the contribution of C−N stretching vibrations) at 1523 cm^{-1} for the lyophilized sample and 1526 cm^{-1} for the film. The thermal properties of BMAP-18A200 film samples were assessed by DSC. The thermogram is characterized by an intense endothermic peak, most likely related to the evaporation of water, starting at the initial temperature (30 °C) and broadening until approximately 120 °C (Figure 4b). Analysis of surface wettability by WCA reveals water contact angles of 75.4°, indicating that the films are hydrophilic (θ < 90°) with relatively good wetting properties (Supporting Figure S5).

Bioactivity of BMAP-18A200 Films. The antimicrobial activity of BMAP-18A200 films was studied against four bacteria and four yeast species by direct contact assay after 120 min of incubation (Figure 4a). The BMAP-18A200 films were highly effective in promoting a killing effect for all the tested microorganisms, achieving a lethality percentage (% of kill) above 95% for all cases. To evaluate if the antimicrobial effect was dependent on the incubation time, the bioactivity of the films was tested through 30 min contact with two skin pathogens of clinical relevance, *S. aureus* (bacterium) and *C. parapsilosis* (yeast) (Figure 4b). Results showed a lethality percentage of 77.42 ± 11.44% for *S. aureus* and 82.86 ± 15.43% for *C. parapsilosis* after 30 min of incubation, whereas these values increase to 98.79 ± 2.0 3% and 100.00% after 120 min of incubation for *S. aureus* and *C. parapsilosis*, respectively. This clearly indicates the time-dependent antimicrobial activity of the BMAP-18A200 films and highlights the strong antimicrobial effect of the material. SEM micrographs of the microorganisms after 120 min of contact with BMAP-18A200 films show irregular cell wall surface, loss of cell shape, and, in some cases, complete disruption resulting in the release of cytoplasmic content (Figure 4c,d). These observations are obvious when considering the micrographs of the control samples (PS disc, Figure 4c,d). To eliminate aberrations deriving from the Au/Pd coating during sample preparation for SEM, micrographs of *P. aeruginosa* were obtained by environmental SEM without any coating. The results reveal the same loss of cell shape, lower cell size, and cell disruption (Supporting Figure S6).

The antimicrobial activity was evaluated against the filamentous fungi *A. nidulans* by inoculating the spores in a solid medium and placing the cast films on top of, or near, the inoculation site (Figure 5a). The films exerted an antifungal effect exclusively by direct contact, as the growth of *A. nidulans* near the BMAP-18A200 films was inhibited, suggesting a lower growth over time when compared to the controls (no sample

https://dx.doi.org/10.1021/acsbiomaterials.0c01262
ACS Biomater. Sci. Eng. XXXX, XXX, XXX−XXX

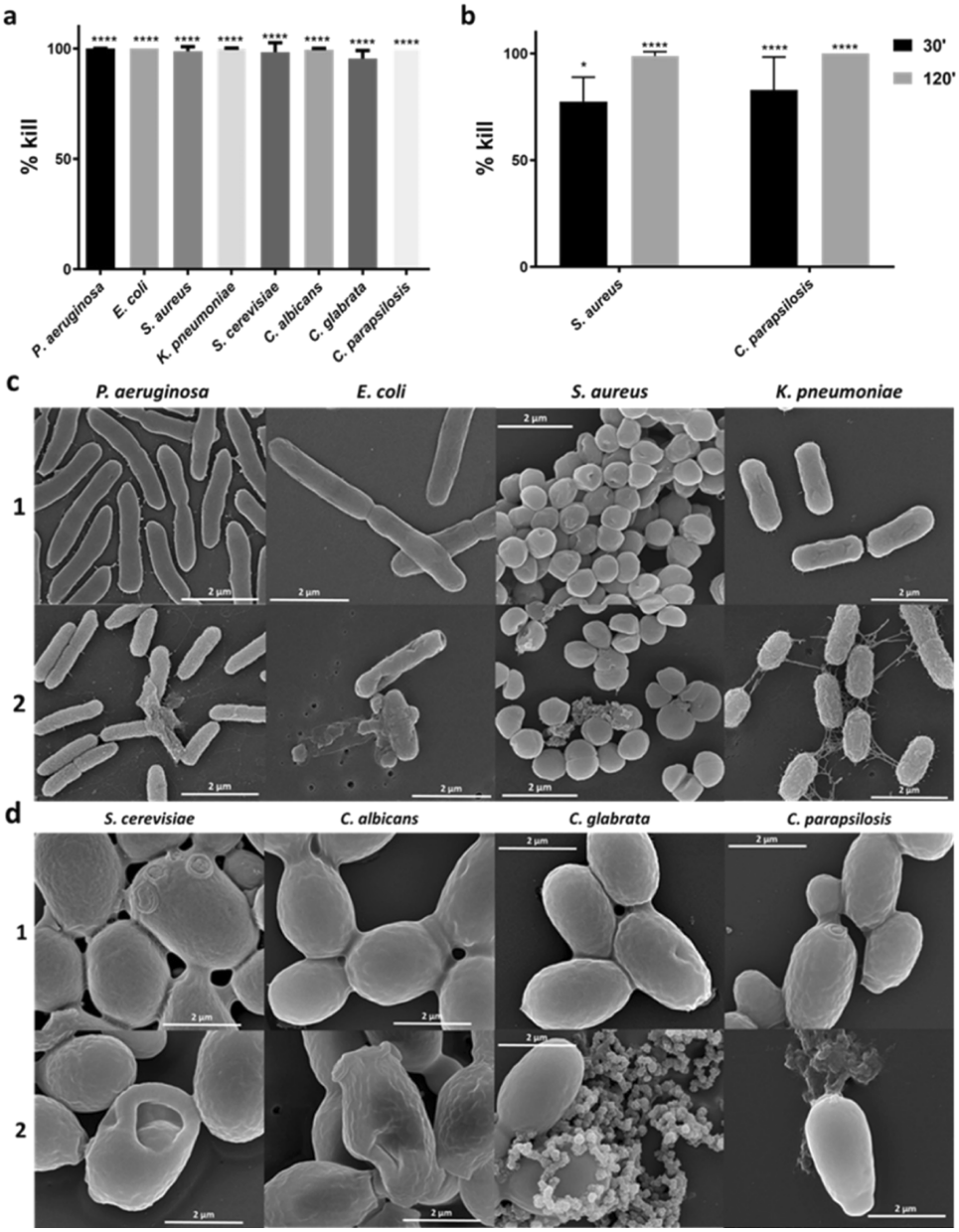

Figure 4. Antimicrobial activity of BMAP-18A200 films by means of an *in vitro* direct contact assay: (a) antimicrobial activity of BMAP-18A200 films against several bacteria and yeasts, after 2 h incubation at 37 and 30 °C, for bacteria and yeast, respectively; (b) Antimicrobial activity of BMAP-18A200 against two skin pathogens at different incubation times. All assays were expressed as % of kill. Sterile PS discs were used as control for survival (set as 100% survival); bars represent means ± SD (*$p \leq 0.05$; ****$p \leq 0.0001$); (c and d) SEM micrographs of different bacterial (c) and yeast (d) species in contact with PS (line 1) and BMAP-18A200 (line 2) surfaces for 120 min, at 37 °C.

and PS disc). This inhibition was even more visible when the film was placed directly on top of the inoculation site resulting in a clear reduction of fungal growth. For a more detailed analysis, hyphae and spore samples in contact with BMAP-18A200 films and PS discs, for 5 and 18 h, were analyzed by SEM (Figure 5b,c). BMAP-18A200 films showed activity not only against the fungal spores but also against the hyphae. In addition to the effective inhibition of spore germination, the films exhibited a fungicidal effect by disrupting the exosporium after 18 h of contact. As for hyphae, the micrographs of samples submitted to 5 h of contact with BMAP-18A200 films clearly show the disruption of cell wall integrity with the presence of numerous pores along the threaded filaments (Figure 5c).

Cytotoxicity Assays. The cytotoxicity of BMAP-18A200 films was evaluated *in vitro* by indirect contact using the MTS cell viability assay and following ISO 10993 recommendations. Cell viability in response to the films was assessed using two different human skin cell lines, BJ-5ta, a normal telomerase-immortalized skin fibroblast cell line, and NCTC 2544, a keratinocyte cell line. Cytotoxicity evaluation on fibroblasts (Figure 6) showed values of 98.2 ± 5.87 and 89.5 ± 6.25% of cell viability after 24 and 72 h, respectively. Similarly, the keratinocytes (Figure 6) reached 96.4 ± 4.34 and 107.3 ± 11.90% of cell viability after 24 and 72 h of contact, respectively. It is worthy to note that the BMAP-18A200 films even induced a slight proliferative effect in keratinocytes after 72 h of contact.

https://dx.doi.org/10.1021/acsbiomaterials.0c01262
ACS Biomater. Sci. Eng. XXXX, XXX, XXX−XXX

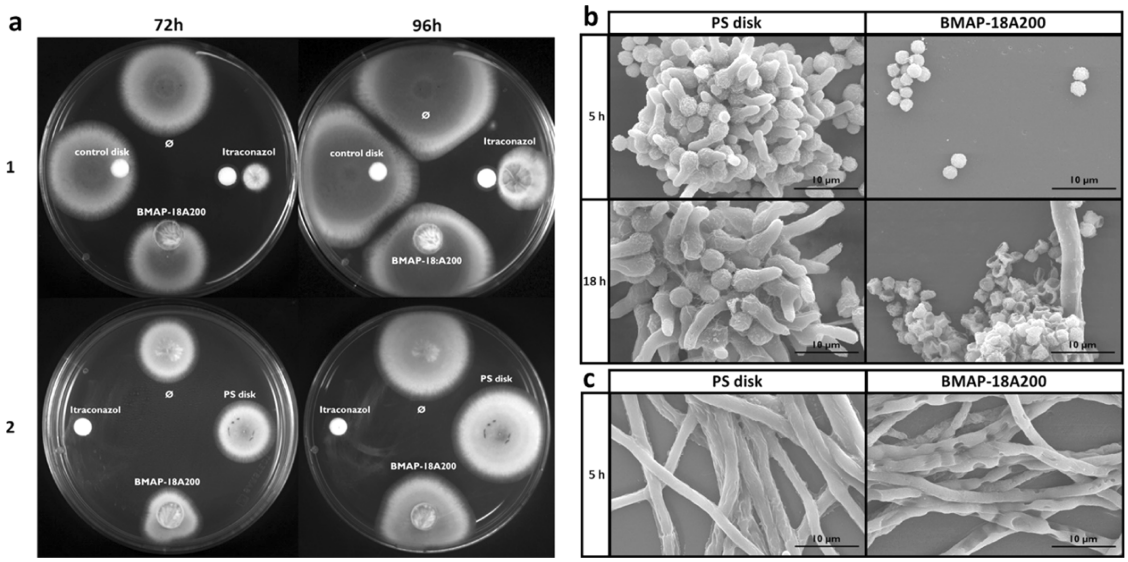

Figure 5. Antifungal activity of BMAP-18A200 films: (a) *A. nidulans* grown in contact with the BMAP-18A200 film, itraconazol-impregnated disc, PS disc, and no sample, for different time points, at 37 °C either with the films near (1) or on top (2) of the inoculation site; (b and c) SEM micrographs of germinating spores (b) and hyphae (c) of *A. nidulans* in contact with PS and BMAP-18A200 discs, for different time points, at 37 °C.

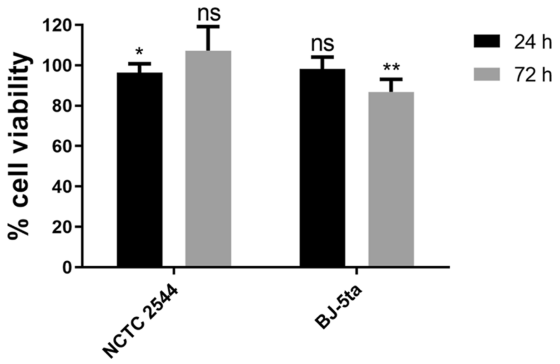

Figure 6. *In vitro* cytotoxicity evaluation of BMAP-18A200 films. Indirect contact MTS cell viability assay on normal human skin fibroblasts (BJ-5ta cell line) and human keratinocytes (NCTC 2544 cell line), after 24 and 48 h of contact with leachables. Results are expressed as % cell viability in relation to the control; bars represent means ± SD (ns, nonsignificant; $*p \leq 0.05$; $**p \leq 0.01$).

■ DISCUSSION

Elastin-like recombinamers have been used for a plethora of different applications including, among others, protein purification, surface engineering, multifunctional materials, drug delivery, and tissue engineering.[13,14,37,38] In this study, we designed an ELR based on 200 repetitions of the pentamer VPAVG (A200) functionalized with the truncated 1−18 amino acid variant (BMAP-18) of the antimicrobial peptide BMAP-28 for the fabrication of antimicrobial free-standing films. Although displaying potent antimicrobial activity, BMAP-28 also displays cytotoxicity against human cells. Works with chemically synthesized BMAP-28 and with the related peptide BMAP-27[27,39−42] report the possibility of amino acidic changes to reduce cytotoxicity without compromising antimicrobial activity. Moreover, Skerlavaj et al. demonstrated that a chemically synthesized variant comprising the first 18 amino acids of BMAP-28 displays no cytotoxicity and possesses great antimicrobial activity.[32] Based on this, we amplified the first 18 amino acids from BMAP-28 sequence to create the truncated variant BMAP-18 to maintain the antimicrobial effect but reduce cytotoxicity to human cells.

Thermal characterization of BMAP-18A200 by DSC indicates that the incorporation of BMAP-18 into the N-terminus of A200 exerts negligible effects on the thermoresponsive behavior of the ELR. The thermograms show the characteristic endothermic peaks of the phase transition with transition temperatures (T_t) in agreement with reference values of A200.[23] Although the hydrophobic folding associated with the phase transition of ELRs is easily achieved by increasing the temperature, the conformational change can also be triggered by increasing the ionic strength (e.g., by adding salt) of the aqueous solution.[23,43,44] This feature is clearly observed in the thermograms depicted in Figure 1a-1. The lower T_t observed for the sample dissolved in PBS is a consequence of the higher ionic strength of the solution. It was suggested that NaCl causes an increase in solvent polarity, and greater differences in polarity in relation to the hydrophobic moieties of the polypeptide result in more ordered water structures surrounding the polymer chain leading to the hydrophobic folding.[23,45] Thus, the salt acts as a "stabilizer" for water molecules and strengthens the intramolecular interactions of the hydrophobic folding. During the cooling stage, the exothermic peak observed in Figure 1a-2 corresponds to the resolubilization of BMAP-18A200 due to the reversibility of the self-assembly process. Again, the effect of the ionic strength in the thermal behavior is clearly observed with BMAP-18A200 showing lower resolubilization temperature values in mQ than in PBS. The acute thermal hysteresis, with differences between the transition temperatures during heating and cooling, is characteristic of the ELRs based on the pentamer VPAVG. This particular behavior is a consequence of the highly stable and compact structure of the self-assembled state formed by intramolecular hydrogen bonding between the amide groups.[23,46,47] The compact structural conformation, derived from the hydrophobic folding with amide groups directly bound together, blocks the penetration of water molecules weakening the possibility of a polymer−

https://dx.doi.org/10.1021/acsbiomaterials.0c01262
ACS Biomater. Sci. Eng. XXXX, XXX, XXX−XXX

water interaction, consequently, resisting more to the reverse dissolution and resulting in the hysteresis behavior.

In addition to the thermal hysteresis found for VPAVG-based ELRs, these unique biopolymers also possess the ability to form spherical or slightly ellipsoidal particle suspensions at temperatures above T_t.[16] As in model ELRs such as poly(VPGVG), A200-based protein polymers form nano- and microparticles that rapidly coalesce to form coacervates.[47] Analysis of the self-assembled BMAP-18A200 structures by DLS demonstrated that both concentration and ionic strength influence the self-assembly process, resulting in distinct patterns. Size measurements with mQ water reveal a homogenous dispersion of populations with size increasing with concentration. On the other hand, size measurements of BMAP-18A200 in PBS reveal an aggregation profile with Z-average values showing a 3- to 8-fold increase when compared to measurements in water. This aggregation profile was previously observed by us with another A200-based protein polymer, namely Hep-A200.[16] We demonstrated that the size of Hep-A200 particles in water is maintained over time but, when in PBS, microaggregates are formed that increase with concentration and time. The dissimilar self-assembly behavior found for water and PBS is thus attributed to the higher ionic strength of the latter and its influence in the hydrophobic folding of BMAP-18A200. Probably, the salts present in the PBS interfere with the hydrophobic moieties of the polymer chain causing a better organization of the hydrophobic folding and is equivalent to an increase in the polymer hydrophobicity resulting in higher packing density (i.e., tighter packing of the ELR chains). Analysis of the particles' ζ-potential in water reveals an increase of this value with concentration. This could be a consequence of the involvement of more polypeptide chains during the self-assembly process, resulting in a greater density of charged BMAP-18A200 per particle. This process can also explain the increase in particle size with concentration. Circular dichroism was employed to study conformational changes in BMAP-18A200; however, due to the low representation of BMAP-18 in the construction of BMAP-18A200 (2.4%), the characteristic α-helix conformation was undetected. Although CD analysis allowed quantification of the secondary structure content at 20 °C (below T_t), this assessment was not possible at 37 °C (above T_t), most likely due to the formation of self-assembled structures that precipitate.

The antimicrobial activity of the films was tested against several microorganisms belonging to the ESKAPE group of pathogens, which represents the most recalcitrant bacteria and is the leading cause of nosocomial infections throughout the world.[48,49] The marginal antibacterial activity of soluble BMAP-18A200 contrast with those obtained with films produced by solvent casting; nonetheless, one must consider that the antimicrobial assays were performed in solution at temperatures above the T_t (37 °C), leading to the formation of self-assembled structures and, therefore, certainly affect the diffusion of BMAP-18A200. SEM micrographs show that the BMAP-18A200 films exerted a microbicidal effect by disrupting cell integrity and consequent release of cytoplasmic content. The formation of transmembrane pores that disrupt cell integrity and result in cell death was previously reported by us for other antimicrobial-functionalized polymers.[13,14] The strong antimicrobial effect of the films was evident even after only 30 min of contact, reaching values above 75% of lethality against the skin pathogens *S. aureus* and *C. parapsilosis*. Altogether, our results demonstrate that the antimicrobial activity of BMAP-18A200 is a time-dependent event, not Gram-related, and is mediated primarily by direct contact.

The occurrence of mold infections in human skin and mucosa is growing, representing a major burden for healthcare units and are associated with high morbidity and severe complications in patients with burns.[50−52] Motivated by the remarkable bioactivity of BMAP-18A200 films, we further extended the antimicrobial assays to the model filamentous fungi, *A. nidulans*. The films promoted the formation of holes along the hyphae compromising its structural integrity, inhibited spore germination, and, inclusively, collapsed the exosporium structure.

DSC analysis of dry films revealed that these are stable over a wide range of temperatures with the detection of a single broad endothermic event, associated with water evaporation. Even in wet conditions, the film demonstrated to maintain its structural integrity (data not shown), dissolving only below its resolubilization temperature, in accordance with BMAP-18A200 thermal hysteresis.

As the aim of the present study was to develop an all protein-based antimicrobial material, inspired by natural proteins, for biomedical applications, cytotoxicity to human cells is a critical parameter. Considering the expected interface with the human body, the cytotoxic response to BMAP-18A200 was evaluated using two human skin cell lines: normal human skin fibroblasts (BJ-5ta) and human keratinocytes (NCTC 2544). Cell viability assays demonstrated lack of toxicity against both cell lines, in accordance to ISO 10993 recommendations, supporting the use of the antimicrobial-functionalized films for skin-related applications (Figure 6). In fact, the NCTC 2544 cells even demonstrated a slight proliferative effect after 72 h of incubation, a result previously attributed to the ELR component.[13,53]

■ CONCLUSIONS

The use of recombinant DNA technology for the creation of functional protein-based materials has the potential to be a game-changing alternative to the traditional chemically synthesized protein polymers. The ability to fine tune the polymeric chain by genetically engineering its sequence and composition allows the fabrication of a multitude of de novo tailor-made multifunctional materials. Herein, we describe the formulation of a highly efficient antimicrobial material by combining in the same polypeptide chain a truncated variant of the antimicrobial peptide BMAP-28 with an elastin-like recombinamer (ELR) based on 200 repetitions of the pentamer VPAVG (A200). The use of A200 provides several advantages: (i) it allows the purification of the functionalized protein by employing simple hot and cold cycles without using harmful chemicals or cumbersome procedures; (ii) it can function as structural and mechanical basis for further processing (e.g., solvent casting); (iii) due to thermal hysteresis, the films are stable at handling temperatures without further cross-linking; and (iv) ELRs are intrinsically biodegradable (composed of amino acids only) and highly biocompatible, encouraging their use for biomedical applications.

Assessment of the antimicrobial performance according to ISO recommendations demonstrated that BMAP-18A200 films were highly effective against clinically relevant microorganisms, including Gram-positive and Gram-negative bacteria as well as unicellular (yeast) and filamentous fungi. The antimicrobial

https://dx.doi.org/10.1021/acsbiomaterials.0c01262
ACS Biomater. Sci. Eng. XXXX, XXX, XXX−XXX

activity of the materials was demonstrated to be exerted through direct contact, promoting microbial cell disruption, as well as compromising the structural integrity of hyphae and spores of filamentous fungi. Finally, it was demonstrated that BMAP-18A200 films are noncytotoxic in *in vitro* cultures of normal human skin fibroblasts and human keratinocytes, validating their potential for safe human use and suggesting these materials as candidates for new drug-free polymers endowed with antimicrobial properties.

In summary, the produced films demonstrated to be stable at handling temperatures without the need for further cross-linking agents while retaining antimicrobial activity. This study thus represents an advance in the formulation and development of bioinspired multifunctional protein-based materials tailored for biomedical applications or even to act as active surfaces and coatings.

■ ASSOCIATED CONTENT

Supporting Information

The Supporting Information is available free of charge at https://pubs.acs.org/doi/10.1021/acsbiomaterials.0c01262.

Schematics of cloning; production and purification; film characterization by SEM, AFM, and contact angle of BMAP-18A200 films; and environmental scanning electronic micrographs showing the antibacterial activity of BMAP-18A200 films against *P. aeruginosa* (PDF)

■ AUTHOR INFORMATION

Corresponding Authors

André da Costa − *CBMA (Centre of Molecular and Environmental Biology), Department of Biology and Institute of Science and Innovation for Bio-Sustainability (IB-S), University of Minho, 4710-057 Braga, Portugal;* orcid.org/0000-0002-4098-2083; Email: andrecosta@bio.uminho.pt

Raul Machado − *CBMA (Centre of Molecular and Environmental Biology), Department of Biology and Institute of Science and Innovation for Bio-Sustainability (IB-S), University of Minho, 4710-057 Braga, Portugal;* orcid.org/0000-0002-9477-9945; Email: raulmachado@bio.uminho.pt

Authors

Ana M. Pereira − *CBMA (Centre of Molecular and Environmental Biology), Department of Biology and Institute of Science and Innovation for Bio-Sustainability (IB-S), University of Minho, 4710-057 Braga, Portugal*

Paula Sampaio − *CBMA (Centre of Molecular and Environmental Biology), Department of Biology and Institute of Science and Innovation for Bio-Sustainability (IB-S), University of Minho, 4710-057 Braga, Portugal*

José Carlos Rodríguez-Cabello − *Bioforge (Group for Advanced Materials and Nanobiotechnology), Centro I+D, Universidad de Valladolid, Valladolid, Spain; Networking Research Centre on Bioengineering, Biomaterials and Nanomedicine (CIBER-BBN), E-47011 Valladolid, Spain*

Andreia C. Gomes − *CBMA (Centre of Molecular and Environmental Biology), Department of Biology and Institute of Science and Innovation for Bio-Sustainability (IB-S), University of Minho, 4710-057 Braga, Portugal*

Margarida Casal − *CBMA (Centre of Molecular and Environmental Biology), Department of Biology and Institute of Science and Innovation for Bio-Sustainability (IB-S), University of Minho, 4710-057 Braga, Portugal*

Complete contact information is available at: https://pubs.acs.org/10.1021/acsbiomaterials.0c01262

Author Contributions

The manuscript was written through contributions of all authors. All authors have given approval to the final version of the manuscript.

Notes

The authors declare no competing financial interest.

■ ACKNOWLEDGMENTS

This work was supported by national funds through FCT I.P. (Fundação para a Ciência e Tecnologia, Portugal) and by the European Regional Development Fund (ERDF) through COMPETE2020—Programa Operacional Competitividade e Internacionalização (POCI, Portugal) in the framework of the Strategic Program UID/BIA/04050/2013 (POCI-01-0145-FEDER-007569). This work was also supported by the strategic program UID/BIA/04050/2019 funded by national funds through FCT I.P. The authors also acknowledge support from FCT I.P. within the ERA-NET IB-2 project FunBioPlas with reference ERA-IB-2-6/0004/2014. AMPereira acknowledges the Doctoral Program in Applied and Environmental Microbiology (DP_AEM), funded by FCT I.P. (grant PD/BD/113811/2015). This article is a result of the project EcoAgriFood (NORTE-01-0145-FEDER-000009), supported by Norte Portugal Regional Operational Programme (NORTE 2020), under the PORTUGAL 2020 Partnership Agreement, through the European Regional Development Fund (ERDF). R.M. acknowledges FCT I.P. for funding in the scope of the Scientific Employment Stimulus instrument (CEECIND/00526/2018).

■ REFERENCES

(1) Cannon, B. Microbiology: Resistance fighters. *Nature* **2014**, *509*, S6−S8.

(2) Stanton, T. B. A call for antibiotic alternatives research. *Trends Microbiol.* **2013**, *21*, 111−113.

(3) Li, X.; Li, P.; Saravanan, R.; Basu, A.; Mishra, B.; Lim, S. H.; Su, X.; Tambyah, P. A.; Leong, S. S. J. Antimicrobial functionalization of silicone surfaces with engineered short peptides having broad spectrum antimicrobial and salt-resistant properties. *Acta Biomater.* **2014**, *10*, 258−266.

(4) Gomes, A. P.; Mano, J. F.; Queiroz, J.; Gouveia, I. C. Incorporation of antimicrobial peptides on functionalized cotton gauzes for medical applications. *Carbohydr. Polym.* **2015**, *127*, 451−461.

(5) Brogden, K. A. Antimicrobial peptides: pore formers or metabolic inhibitors in bacteria? *Nat. Rev. Microbiol.* **2005**, *3*, 238−250.

(6) Cotter, P. D.; Ross, R. P.; Hill, C. Bacteriocins - a viable alternative to antibiotics? *Nat. Rev. Microbiol.* **2013**, *11*, 95−105.

(7) Wang, G.; Mishra, B.; Lau, K.; Lushnikova, T.; Golla, R.; Wang, X. Antimicrobial Peptides in 2014. *Pharmaceuticals* **2015**, *8*, 123−150.

(8) Deng, T.; Ge, H.; He, H.; Liu, Y.; Zhai, C.; Feng, L.; Yi, L. The heterologous expression strategies of antimicrobial peptides in microbial systems. *Protein Expression Purif.* **2017**, *140*, 52−59.

(9) Sinha, R.; Shukla, P. Antimicrobial Peptides: Recent Insights on Biotechnological Interventions and Future Perspectives. *Protein Pept. Lett.* **2019**, *26*, 79−87.

(10) Li, Y. Recombinant Production of Antimicrobial Peptides in Escherichia coli: A Review. *Protein Expression Purif.* **2011**, *80*, 260−267.

(11) Ingham, A. B.; Moore, R. J. Recombinant production of antimicrobial peptides in heterologous microbial systems. *Biotechnol. Appl. Biochem.* **2007**, *47*, 1.

(12) Hu, F.; Ke, T.; Li, X.; Mao, P. H.; Jin, X.; Hui, F. L.; Ma, X. D.; Ma, L. X. Expression and purification of an antimicrobial peptide by fusion with elastin-like polypeptides in Escherichia coli. *Appl. Biochem. Biotechnol.* **2010**, *160*, 2377−2387.

(13) da Costa, A.; Machado, R.; Ribeiro, A.; Collins, T.; Thiagarajan, V.; Neves-Petersen, M. T.; Rodríguez-Cabello, J. C.; Gomes, A. C.; Casal, M. Development of Elastin-Like Recombinamer Films with Antimicrobial Activity. *Biomacromolecules* **2015**, *16*, 625−635.

(14) da Costa, A.; Pereira, A. M.; Gomes, A. C.; Rodriguez-Cabello, J. C.; Sencadas, V.; Casal, M.; Machado, R. Single step fabrication of antimicrobial fibre mats from a bioengineered protein-based polymer. *Biomed. Mater.* **2017**, *12*, No. 045011.

(15) Yang, K.; Su, Y.; Li, J.; Sun, J.; Yang, Y. Expression and purification of the antimicrobial peptide cecropin AD by fusion with cationic elastin-like polypeptides. *Protein Expression Purif.* **2012**, *85*, 200−203.

(16) da Costa, A.; Pereira, A. M.; Gomes, A. C.; Rodriguez-Cabello, J. C.; Casal, M.; Machado, R. Production of bioactive hepcidin by recombinant DNA tagging with an elastin-like recombinamer. *New Biotechnol.* **2018**, *46*, 45−53.

(17) Hassouneh, W.; Christensen, T.; Chilkoti, A. Elastin-Like Polypeptides as a Purification Tag for Recombinant Proteins. In *Current Protocols in Protein Science*; John Wiley & Sons, Inc.: Hoboken, NJ, 2010; pp 6.11.1−6.11.16.

(18) Girotti, A.; Fernández-Colino, A.; López, I. M.; Rodríguez-Cabello, J. C.; Arias, F. J. Elastin-like recombinamers: biosynthetic strategies and biotechnological applications. *Biotechnol. J.* **2011**, *6*, 1174−1186.

(19) Rodriguez-Cabello, J. C. Smart elastin-like polymers. In *Advances in Experimental Medicine and Biology*; Springer: Boston, MA, 2004; Vol. *553*, pp 45−57.

(20) Nettles, D. L.; Chilkoti, A.; Setton, L. A. Applications of elastin-like polypeptides in tissue engineering. *Adv. Drug Delivery Rev.* **2010**, *62*, 1479.

(21) Simnick, A. J.; Lim, D. W.; Chow, D.; Chilkoti, A. Biomedical and Biotechnological Applications of Elastin-Like Polypeptides. *Polym. Rev.* **2007**, *47*, 121−154.

(22) Rincón, A. C.; Molina-Martinez, I. T.; de las Heras, B.; Alonso, M.; Baílez, C.; Rodríguez-Cabello, J. C.; Herrero-Vanrell, R. Biocompatibility of elastin-like polymer poly(VPAVG) microparticles: in vitro and in vivo studies. *J. Biomed. Mater. Res. Part A* **2006**, *78A*, 343−351.

(23) Machado, R.; Ribeiro, A. J.; Padrão, J.; Silva, D.; Nobre, A.; Teixeira, J. A.; Arias, F. J.; Cunha, A. M.; Rodríguez-Cabello, J. C.; Casal, M. Exploiting the Sequence of Naturally Occurring Elastin: Construction, Production and Characterization of a Recombinant Thermoplastic Protein-Based Polymer. *J. Nano Res.* **2009**, *6*, 133−145.

(24) Herrero-Vanrell, R.; Rincón a, C.; Alonso, M.; Reboto, V.; Molina-Martinez, I. T.; Rodríguez-Cabello, J. C. Self-assembled particles of an elastin-like polymer as vehicles for controlled drug release. *J. Controlled Release* **2005**, *102*, 113−122.

(25) Arau'jo, R.; Silva, C.; Machado, R.; Casal, M.; Cunha, A. M.; Rodriguez-Cabello, J. C.; Cavaco-Paulo, A. Proteolytic Enzyme Engineering: A Tool for Wool. *Biomacromolecules* **2009**, *10*, 1655−1661.

(26) Machado, R.; Bessa, P. C.; Reis, R. L.; Rodriguez-Cabello, J. C.; Casal, M. Elastin-Based Nanoparticles for Delivery of Bone Morphogenetic Proteins. In *Nanoparticles in Biology and Medicine*; Humana Press: Totowa, NJ, 2012; Vol. *906*, pp 353−363.

(27) Risso, A.; Braidot, E.; Sordano, M. C.; Vianello, A.; Macrı, F.; Skerlavaj, B.; Zanetti, M.; Gennaro, R.; Bernardi, P. BMAP-28, an Antibiotic Peptide of Innate Immunity, Induces Cell Death through Opening of the Mitochondrial Permeability Transition Pore. *Mol. Cell. Biol.* **2002**, *22*, 1926−1935.

(28) Ahmad, A.; Asthana, N.; Azmi, S.; Srivastava, R. M.; Pandey, B. K.; Yadav, V.; Ghosh, J. K. Structure-function study of cathelicidin-derived bovine antimicrobial peptide BMAP-28: design of its cell-selective analogs by amino acid substitutions in the heptad repeat sequences. *Biochim. Biophys. Acta* **2009**, *1788*, 2411−2420.

(29) Zanetti, M. The role of cathelicidins in the innate host defenses of mammals. *Curr. Issues Mol. Biol.* **2005**, *7*, 179−196.

(30) Brogden, K. A.; Nordholm, G.; Ackermann, M. Antimicrobial activity of cathelicidins BMAP28, SMAP28, SMAP29, and PMAP23 against Pasteurella multocida is more broad-spectrum than host species specific. *Vet. Microbiol.* **2007**, *119*, 76−81.

(31) Risso, A.; Zanetti, M.; Gennaro, R. Cytotoxicity and apoptosis mediated by two peptides of innate immunity. *Cell. Immunol.* **1998**, *189*, 107−115.

(32) Skerlavaj, B.; Gennaro, R.; Bagella, L.; Merluzzi, L.; Risso, A.; Zanettit, M. Biological characterization of two novel cathelicidin-derived peptides and identification of structural requirements for their antimicrobial and cell lytic activities. *J. Biol. Chem.* **1996**, *271*, 28375−28381.

(33) Wang, G.; Li, X.; Wang, Z. APD3: The antimicrobial peptide database as a tool for research and education. *Nucleic Acids Res.* **2016**, *44*, D1087.

(34) Micsonai, A.; Wien, F.; Bulyáki, É.; Kun, J.; Moussong, É.; Lee, Y. H.; Goto, Y.; Réfrégiers, M.; Kardos, J. BeStSel: A web server for accurate protein secondary structure prediction and fold recognition from the circular dichroism spectra. *Nucleic Acids Res.* **2018**, *46*, W315−22.

(35) Schneider, C. A.; Rasband, W. S.; Eliceiri, K. W. NIH Image to ImageJ: 25 years of image analysis. *Nat. Methods* **2012**, *9*, 671−675.

(36) McPherson, D. T.; Morrow, C.; Minehan, D. S.; Wu, J.; Hunter, E.; Urry, D. W. Production and purification of a recombinant elastomeric polypeptide, G-(VPGVG)19-VPGV, from Escherichia coli. *Biotechnol. Prog.* **1992**, *8*, 347−352.

(37) Ibáñez-Fonseca, A.; Flora, T.; Acosta, S.; Rodríguez-Cabello, J. C. Trends in the design and use of elastin-like recombinamers as biomaterials. *Matrix Biol.* **2019**, *84*, 111.

(38) Rodríguez-Cabello, J. C.; Arias, F. J.; Rodrigo, M. A.; Girotti, A. Elastin-like polypeptides in drug delivery. *Adv. Drug Delivery Rev.* **2016**, *97*, 85−100.

(39) Haines, L. R.; Thomas, J. M.; Jackson, A. M.; Eyford, B. A.; Razavi, M.; Watson, C. N.; Gowen, B.; Hancock, R. E. W.; Pearson, T. W. Killing of trypanosomatid parasites by a modified bovine host defense peptide, BMAP-18. *PLoS Negl. Trop. Dis.* **2009**, *3*, No. e373.

(40) Lee, E. K.; Kim, Y.-C.; Nan, Y. H.; Shin, S. Y. Cell selectivity, mechanism of action and LPS-neutralizing activity of bovine myeloid antimicrobial peptide-18 (BMAP-18) and its analogs. *Peptides* **2011**, *32*, 1123−1130.

(41) Mardirossian, M.; Pompilio, A.; Crocetta, V.; De Nicola, S.; Guida, F.; Degasperi, M.; Gennaro, R.; Di Bonaventura, G.; Scocchi, M. In vitro and in vivo evaluation of BMAP-derived peptides for the treatment of cystic fibrosis-related pulmonary infections. *Amino Acids* **2016**, *48*, 2253−2260.

(42) D'Este, F.; Oro, D.; Boix-Lemonche, G.; Tossi, A.; Skerlavaj, B. Evaluation of free or anchored antimicrobial peptides as candidates for the prevention of orthopaedic device-related infections. *J. Pept. Sci.* **2017**, *23*, 777−789.

(43) Cho, Y.; Zhang, Y.; Christensen, T.; Sagle, L. B.; Chilkoti, A.; Cremer, P. S. Effects of hofmeister anions on the phase transition temperature of elastin-like polypeptides. *J. Phys. Chem. B* **2008**, *112*, 13765−13771.

(44) Park, J. E.; Won, J. I. Thermal behaviors of elastin-like polypeptides (ELPs) according to their physical properties and environmental conditions. *Biotechnol. Bioprocess Eng.* **2009**, *14*, 662.

(45) Reguera, J.; Urry, D. W.; Parker, T. M.; McPherson, D. T.; Rodríguez-Cabello, J. C. Effect of NaCl on the exothermic and endothermic components of the inverse temperature transition of a model elastin-like polymer. *Biomacromolecules* **2007**, *8*, 354−358.

(46) Reguera, J.; Lagarón, J. M.; Alonso, M.; Reboto, V.; Calvo, B.; Rodríguez-Cabello, J. C. Thermal Behavior and Kinetic Analysis of

https://dx.doi.org/10.1021/acsbiomaterials.0c01262
ACS Biomater. Sci. Eng. XXXX, XXX, XXX−XXX

the Chain Unfolding and Refolding and of the Concomitant Nonpolar Solvation and Desolvation of Two Elastin-like Polymers. *Macromolecules* **2003**, *36*, 8470−8476.

(47) Schmidt, P.; Dybal, J.; Rodriguez-Cabello, J. C.; Reboto, V. Role of water in structural changes of poly(AVGVP) and poly-(GVGVP) Studied by FTIR and Raman spectroscopy and ab initio calculations. *Biomacromolecules* **2005**, *6*, 697−706.

(48) Mulani, M. S.; Kamble, E. E.; Kumkar, S. N.; Tawre, M. S.; Pardesi, K. R. Emerging Strategies to Combat ESKAPE Pathogens in the Era of Antimicrobial Resistance: A Review. *Front. Microbiol.* **2019**, *10*, 539.

(49) Pendleton, J. N.; Gorman, S. P.; Gilmore, B. F. Clinical relevance of the ESKAPE pathogens. *Expert Rev. Anti. Infect. Ther.* **2013**, *11*, 297−308.

(50) Kotwal, A.; Biswas, D.; Kakati, B.; Roy, S.; Chauhan, B. S. *Aspergillus nidulans* causing primary cutaneous aspergillosis in an immunocompetent patient. *Cutis* **2015**, *95*, E1−E3.

(51) Guégan, S.; Lanternier, F.; Rouzaud, C.; Dupin, N.; Lortholary, O. Fungal skin and soft tissue infections. *Curr. Opin. Infect. Dis.* **2016**, *29*, 124−130.

(52) Tatara, A. M.; Mikos, A. G.; Kontoyiannis, D. P. Factors affecting patient outcome in primary cutaneous aspergillosis. *Medicine* **2016**, *95*, No. e3747.

(53) Bessa, P. C.; Machado, R.; Nürnberger, S.; Dopler, D.; Banerjee, A.; Cunha, A. M.; Rodríguez-Cabello, J. C.; Redl, H.; van Griensven, M.; Reis, R. L.; Casal, M. Thermoresponsive self-assembled elastin-based nanoparticles for delivery of BMPs. *J. Controlled Release* **2010**, *142*, 312−318.

https://dx.doi.org/10.1021/acsbiomaterials.0c01262
ACS Biomater. Sci. Eng. XXXX, XXX, XXX−XXX